J. Phys. B: Atom. Molec. Phys. **13** (1980) 2633–2643. Printed in Great Britain

Elastic and inelastic scattering of electrons by Na†

S K Srivastava and L Vušković‡

Jet Propulsion Laboratory, California Institute of Technology, Pasadena, California 91103, USA

Received 16 July 1979, in final form 18 December 1979

Abstract. Utilising a crossed-electron-beam–metal-atom-beam scattering technique differential excitation cross sections at 10, 20, 40, and 54·4 eV incident energies and at scattering angles ranging from 10 to 120° have been measured for the following transitions: (i) elastic scattering, and (ii) excitation from ground state (3^2S) to (*a*) 3^2P, (*b*) 4^2S, (*c*) 3^2D+4^2P and (*d*) $4^2D+4^2F+5^2P+5^2S$ states in Na. Comparisons with recent theoretical and experimental results have been made. Using previous theoretical and experimental results as guides the present differential cross sections have been extrapolated between angular regions of 0–10° and 120–180°. Integral and momentum cross sections have been computed from these cross sections.

1. Introduction

The recent discovery of sodium in the atmosphere of Io has initiated our interest in the measurement of electron impact excitation cross sections of Na. Such cross sections are also important for the purpose of modelling the plasma of several electrical discharges containing sodium. Sodium is also of interest from the theoretical point of view. Its electronic configuration is similar to that of the hydrogen atom. Its core is inert with a single valence electron. Therefore, it is natural to expect that the cross sections for single-electron excitation should resemble those for hydrogen. However, this is not so. First, the size of the Na atom is larger than hydrogen and hence has larger electron scattering cross sections. Second, the first excited state is only 2·1 eV above the ground state as opposed to 10·2 eV for hydrogen. Consequently, the polarisability of the Na atom is much larger than that of the hydrogen atom. These facts require a much more sophisticated theoretical treatment of the Na atom than of the hydrogen atom.

Although alkali metals have received much attention in the past and a large amount of scattering data exist, there are only a few measurements (Teubner *et al* 1978, Gehenn and Reichert 1972, Shuttleworth *et al* 1977a) on the differential cross sections (DCS) for Na for electron impact energies lying between the threshold of excitation and 100 eV. Such cross sections are important because they yield momentum transfer cross sections which are useful in Na plasma modelling.

Almost all previous experimental and theoretical works on e–Na collision cross sections have been summarised in a review paper by Bransden and McDowell (1978) and comparisons between various theories and experiments can be found there.

† Research supported in part by NASA Contract No NAS7-100 Office of Space Sciences and partially by the California Institute of Technology through the Caltech President's fund.

‡ NRC/NASA Senior Resident Research Associate; permanent address: Institute of Physics, PO Box 57, Belgrade, Yugoslavia.

0022-3700/80/132633+11$01.50

In this paper we present differential, integral, and momentum transfer cross sections for electron impact energies of 10, 20, 40 and 54·4 eV. These cross sections have been measured for elastic scattering and for the excitation of the following states: (*a*) 3^2P, (*b*) 4^2S, (*c*) 3^2D+4^2P and (*d*) $4^2D+4^2F+5^2P+5^2S$.

2. Apparatus and method

The apparatus used in the present measurements has been described in detail in a previous publication (Trajmar *et al* 1977). Briefly, a crossed-electron-beam–atom-beam scattering geometry was employed. A monoenergetic beam of electrons of desired incident energy was produced by heating a tungsten filament and passing the thermionically emitted electrons through a set of cylindrical electron lenses and a hemispherical energy analyser. In the present experiment the overall resolution of the spectrometer was about 80 mV. The beam of sodium atoms was generated by resistive heating of a stainless steel crucible. In order to avoid the effects of magnetic fields a coaxial heating wire was wrapped around the crucible. The temperature of the crucible was not measured. Instead, it was heated to the point where the Na density in the atomic beam was high enough to observe sufficient electron scattering. However, from our previous calibrations and from the amount of steady state current flowing through the coaxial heating wires it was estimated that the temperature of the crucible was about 400 °C. The steady state value of the current did not change during the entire experiment which indicated that the temperature of the crucible was constant. Scattered electrons passed through a hemispherical energy analyser which determined the energy lost by them. These electrons were detected by a spiraltron and were counted by a conventional pulse amplification and multichannel scaling technique.

Commercial sodium preserved in kerosene oil was cut into small pieces and then placed in the stainless steel crucible. Since the sodium was contaminated with oil, the crucible was heated slowly over a period of a few hours to avoid the sudden evaporation of the oil. During this time the background pressure in the vacuum chamber was monitored by an ionisation gauge. As the temperature of the crucible was increased, it was observed that the background pressure rose (to about 2×10^{-5} Torr) until all the oil evaporated at which point the background pressure resumed its original value ($\simeq2\times10^{-7}$ Torr). This precaution was very important; otherwise the scattered intensity would be due to both sodium and oil. Under these conditions it was found that the scattering due to background was negligible in comparison with the scattering signal from the atomic beam.

In the present experimental arrangement the electron gun was rotated around the beam of Na atoms and the detector was kept fixed. Due to certain physical limitations the maximum scattering angle at which the intensity could be recorded was 120°. The scattered electron signal intensity is related to the differential cross section (DCS) by the following relation:

$$I(\theta)=K(\theta)\,(\mathrm{DCS})\,P \tag{1}$$

where P is a constant and does not depend on scattering angle θ. $K(\theta)$ is a geometrical factor which at low scattering angles strongly depends on θ. $K(\theta)$ can be calculated if the geometry of the overlapping region formed by the electron beam, atom beam, and the solid angle of the detector are known accurately. It has generally been found that for scattering angles larger than 30° the factor $K(\theta)$ can be replaced by sin θ. However,

as pointed out by Shuttleworth *et al* (1977a) this may not be true for all scattering geometries. A recent comprehensive study of this subject (Trajmar and Brinkmann 1979) shows that $K(\theta)$ can be significantly different from $\sin\theta$ for some scattering geometries. Using the results of Trajmar and Brinkmann (1979) we calculated the values of $K(\theta)$ for the present set-up and corrected the scattered electron intensity to represent the variation of DCS with the scattering angle.

The scattered electron intensity could also be affected by the presence of Na_2 and multiple scattering. At the vapour pressure and temperatures encountered during the present measurements the presence of Na_2 could be ruled out. Multiple scattering can occur if the mean free path of the electron is smaller than or comparable to the target size. It could be recognised by the occurrence of an energy-loss feature at twice the energy loss of the corresponding single scattering inelastic feature (Williams and Trajmar 1977). No such scattering feature was seen in the spectra.

The method of data reduction was as follows. First, energy-loss spectra at incident energies of 10, 20, 40 and 54·4 eV and for scattering angles varying from 10° to 120° were recorded several times. Three typical energy-loss spectra at scattering angles of 10, 30 and 80° and for incident energy of 20 eV are shown in figure 1. Second, from these spectra ratios of elastic and all inelastic features with respect to the spectral feature corresponding to $3^2S \rightarrow 3^2P$ were determined. Third, the distribution of the intensity of $3^2S \rightarrow 3^2P$ feature with respect to scattering angle θ was determined. This angular distribution was then corrected for the geometrical factor $K(\theta)$ as described above.

The corrected intensity distribution of $3^2S \rightarrow 3^2P$ transition was directly proportional to the differential cross section (DCS). These DCS were measured for the angular range of 10° to 120°. Between 0° and 10° and between 120° and 180° extrapolations were made by using the relative shapes of the DCS curves predicted by Kennedy *et al* (1977). The relative values of the differential cross sections were then employed to calculate integral cross sections in arbitrary units (equation (2)) which were subsequently put on the absolute scale by using the optical excitation functions of Enemark and Gallagher (1972). The normalisation factor, so obtained, was used to determine absolute values of the DCS for the $3^2S \rightarrow 3^2P$ transition.

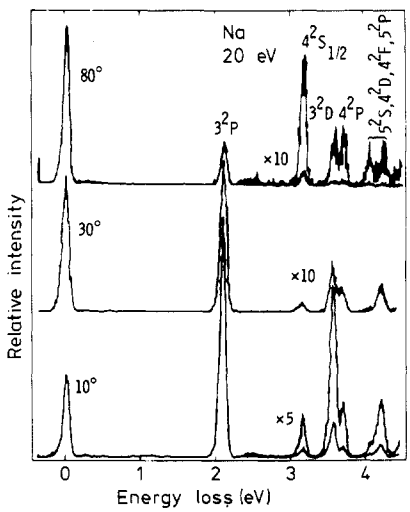

Figure 1. Energy-loss spectra of Na at 20 eV electron impact energy and scattering angles of 10, 30 and 80°.

The ratios of various inelastic transitions and of elastic scattering with respect to $3^2S \rightarrow 3^2P$ transitions were then multiplied by the DCS values as obtained above. These provided absolute cross sections for other transitions.

3. Results and discussion

The differential cross sections obtained by the method described in the previous section are presented in tables 1–5. The relative values of cross sections for individual transitions at a particular incident energy are estimated to be accurate to within ±10%. The errors in the absolute values have been estimated by taking into account the errors in the normalisation procedure. The error in the absolute value of the integral cross section of $3^2S \rightarrow 3^2P$ measured by Enemark and Gallagher (1972) used for normalisation of this data has been given to be approximately 5%. About 15% error is introduced by the extrapolation which is made between 0 to 10° and 120 to 180° in order to obtain the integral cross sections. Thus the combined error, calculated by taking the square root of the sum of the squares of individual errors, is about 20% for the $3^2S \rightarrow 3^2P$ DCS. For the cross sections for elastic scattering and other inelastic excitations there is an added error which arises due to the efficiency of the electron energy analyser optics. The efficiency of detection may change from transition to transition. Therefore, the ratio of elastic intensity or the intensity of other inelastic features with respect to the intensity of resonance ($3^2S \rightarrow 3^2P$) feature may be in error due to a different detection efficiency. This error has been estimated to be 10%. Thus, the total estimated error in the cross section values of elastic scattering and other

Table 1. Elastic DCS of Na in the units of 10^{-16} cm^2 sr^{-1}. Error in the values of cross sections is estimated to be 22%. σ_I and σ_M have been estimated to be in error by about 30% and 35% respectively.

θ (deg) \ E_0 (eV)	10	20	40	54·4
10	115	22	16	6·7
15	43	11	7·2	3·1
20	19	5·0	3·8	1·3
30	3·5	0·70	1·1	0·34
40	0·64	0·15	0·52	0·19
50	0·094	0·20	0·45	0·16
60	0·24	0·30	0·45	0·12
70	0·41	0·34	0·38	0·093
80	0·61	0·36	0·28	0·062
90	0·69	0·31	0·17	0·034
100	0·61	0·22	0·070	0·011
110	0·44	0·12	0·030	0·0047
120	0·30	0·063	0·031	0·022
Integral 10^{-16} cm^2	43	14	11	5·4
Momentum 10^{-16} cm^2	7·1	2·62	2·0	0·82

Table 2. DCS for the $3^2S \rightarrow 3^2P$ transition in Na in units of 10^{-16} cm^2 sr^{-1}. The values are uncertain by about 20%. σ_M are estimated to be in error by about 35%.

θ (deg) \ E (eV)	10	20	40	54·4
10	99	46	40	11
15	21	21	13	1·5
20	14	6·7	3·4	0·33
30	4·3	0·86	0·36	0·036
40	1·2	0·24	0·13	0·013
50	0·54	0·048	0·063	0·0078
60	0·19	0·042	0·050	0·0091
70	0·14	0·061	0·050	0·0080
80	0·12	0·086	0·037	0·0078
90	0·15	0·093	0·030	0·0049
100	0·21	0·086	0·014	0·0033
110	0·14	0·056	0·0059	0·0014
120	0·057	0·031	0·011	0·0062
Integral† 10^{-16} cm^2	31·7	29·0	21·8	18·6
Momentum 10^{-16} cm^2	7·7	6·4	4·4	3·5

† Enemark and Gallagher (1972). The values quoted here have been obtained by interpolating their results.

Table 3. DCS for the $3^2S \rightarrow 4^2S$ transition in Na in units of 10^{-16} cm^2 sr^{-1}. The error estimates are same as in table 1.

θ (deg) \ E (eV)	10	20	40	54·4
10	1·2	0·84	1·3	0·41
15	0·72	0·50	0·53	0·065
20	0·51	0·29	0·18	0·024
30	0·19	0·070	0·058	0·016
40	0·098	0·031	0·031	0·010
50	0·040	0·0077	0·032	0·0067
60	0·026	0·019	0·023	0·0049
70	0·024	0·022	0·015	0·0043
80	0·040	0·024	0·011	0·0019
90	0·054	0·025	0·0071	0·0012
100	0·063	0·018	0·0038	0·00044
110	0·041	0·0064	0·00090	0·00017
120	0·012	0·0022	0·00043	0·0013
Integral 10^{-16} cm^2	1·0	0·524	0·58	0·30
Momentum 10^{-16} cm^2	0·51	0·30	0·14	0·57

Table 4. DCS for the $3^2S \rightarrow 3^2D + 4^2P$ transition in Na in units of 10^{-16} cm^2 sr^{-1}. The error estimates are same as in table 1.

θ (deg) \ E (eV)	10	20	40	54·4
10	6·7	5·0	6·7	2·7
15	4·7	3·3	3·5	0·66
20	3·4	1·9	1·3	0·16
30	1·4	0·37	0·12	0·012
40	0·37	0·084	0·039	0·0052
50	0·14	0·018	0·021	0·0052
60	0·083	0·012	0·013	0·0039
70	0·065	0·018	0·0096	0·0026
80	0·045	0·019	0·0077	0·0016
90	0·043	0·024	0·0056	0·0012
100	0·058	0·022	0·0036	0·00089
110	0·041	0·013	0·0014	0·00054
120	0·018	0·0084	0·0028	0·0022
Integral 10^{-16} cm^2	4·3	2·4	2·4	0·97
Momentum 10^{-16} cm^2	1·4	0·93	0·53	0·19

Table 5. DCS for the transition $3^2S \rightarrow 4^2D + 4^2F + 5^2P + 5^2S$ in Na in units of 10^{-16} cm^2 sr^{-1}. The error estimates are same as in table 1.

θ (deg) \ E (eV)	10	20	40	54·4
10	1·9	1·5	2·0	0·87
15	1·4	1·3	1·6	0·28
20	1·0	0·98	0·54	0·073
30	0·52	0·19	0·070	0·0094
40	0·16	0·048	0·028	0·0036
50	0·062	0·0077	0·018	0·0025
60	0·051	0·0091	0·012	0·0028
70	0·041	0·012	0·0077	0·0023
80	0·037	0·013	0·0046	0·0017
90	0·031	0·014	0·0032	0·0012
100	0·059	0·018	0·0021	0·00089
110	0·033	0·0052	0·00071	0·00034
120	0·014	0·0025	0·00067	0·00078
Integral 10^{-16} cm^2	1·6	0·97	0·87	0·30
Momentum 10^{-16} cm^2	0·65	0·40	0·21	0·066

inelastic features besides the resonance transition ($3^2S \rightarrow 3^2P$) is about 22%. This is the square root of the sum of squares of 20% error in the cross section for the resonance transition and 10% error due to uncertainty in the ratios of elastic and other inelastic intensities to the intensity of the resonance transition.

The present results are compared with the theoretical results of Issa (1977) and the experimental values of Gehenn and Reichert (1972) at 10 eV incident energy for the elastic scattering (figure 2). The results of Gehenn and Reichert are in relative units and have been normalised to the present results at 90°. The shapes of the two curves agree fairly well at high scattering angles but at low angles they differ. Theoretical calculations of Issa using the full partial-wave close coupling method and including exchange and the second-order potential in the elastic channel give values which agree with the present results within a factor of two. However, the normalised values of Gehenn and Reichert are in better agreement with the theory. In the case of $3^2S \rightarrow 3^2P$ transition (figure 3) Issa's results are in excellent agreement with the present ones at low scattering angles. Figure 3 also includes the results of the distorted-wave polarised orbital calculations of Kennedy *et al* (1977). At high scattering angles the present results lie between the two theoretical predictions. However, the shape of the present curve follows the shape of Issa's calculations.

At the higher impact energy of 54·4 eV the recent measurements of Teubner *et al* (1978) for elastic and of S J Buckman and P J O Teubner (1978, private communication) for the resonance transition are available. They are compared with the present results in figures 4 and 5 for elastic and for $3^2S \rightarrow 3^2P$ transitions respectively. In the past, calculations utilising Born, Glauber, distorted-wave, close coupling approximations have been performed and details on them can be found in the review paper by

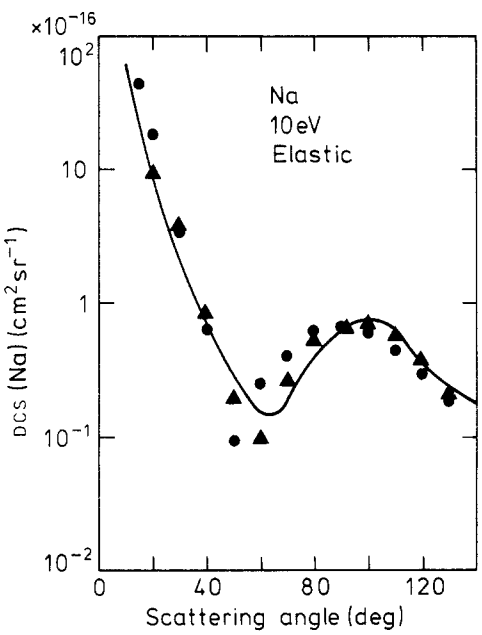

Figure 2. DCS for elastic scattering of 10 eV electrons by Na. ▲, Gehenn and Reichert (these relative values are normalised to ours at 90°) (1972); ——, Issa (1977); ●, present results.

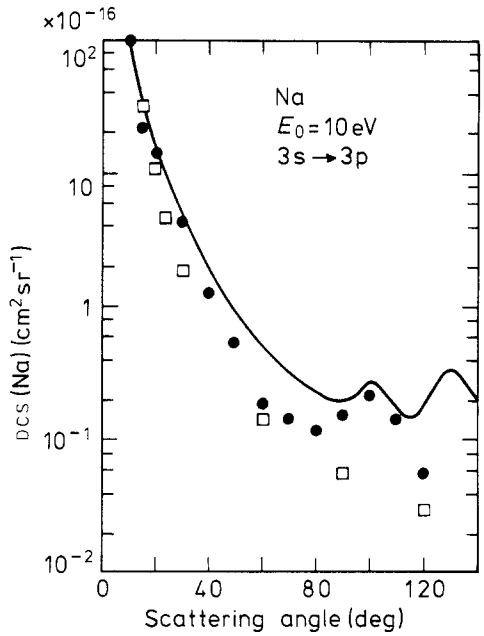

Figure 3. DCS for $3^2S \rightarrow 3^2P$ excitation for 10 eV electrons in Na. ——, Issa (1977); □, Kennedy *et al* (1977); ●, present results.

Bransden and McDowell (1978). In figure 4 we have compared present results ($E_0 = 54{\cdot}4$ eV) with recent calculations of Issa (1977) ($E_0 = 50$ eV) which use the second-order potentials of Bransden and Coleman (1972) to estimate the effects of the states not explicitly included in a two-state close coupling approximation. The agreement of this theory with the present results at low scattering angles is excellent but at high scattering angles the differences are rather large. However, the qualitative shapes of the two curves are similar. Figure 4 also contains the predictions of the optical model calculations of Teubner *et al* (1978). Within the error limits of the present measurements the agreement with this theory is good for angles up to about 40°. A comparison with the experimental results of Teubner *et al* (1978) reveals a similar situation. These differences at large scattering angles between the two measurements are a matter of concern. The shapes of the differential cross section curves can be distorted if proper account is not taken of the geometrical correction factor given by equation (1). In the present experiment this factor was carefully calculated and it is estimated that the relative shape of the present DCS curve is not in error by more than ±10%. Figure 5 compares the measurements of S J Buckman and P J O Teubner (1978, private communication) and Shuttleworth *et al* (1977a) with the present results. Also included are the unitarised distorted-wave polarised orbital calculations of Kennedy *et al* (1977) and close coupling calculations of Issa (1977) ($E_0 = 50$ eV). It is clear from this figure that the agreement between the various results is within their error limits for low scattering angles. However, at larger scattering angles the differences are appreciable once again, similar to those shown in figure 4. Of the two theories, DWPO predicts

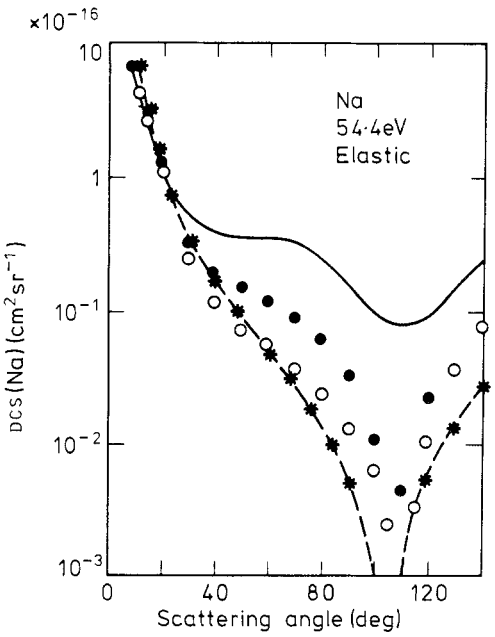

Figure 4. DCS for elastic scattering of 54·4 eV electrons by Na. ○, Teubner *et al* (1978) (experiment) and – – * – –, Teubner *et al* (optical model potential); ——, Issa (1977) (50 eV); ●, present results.

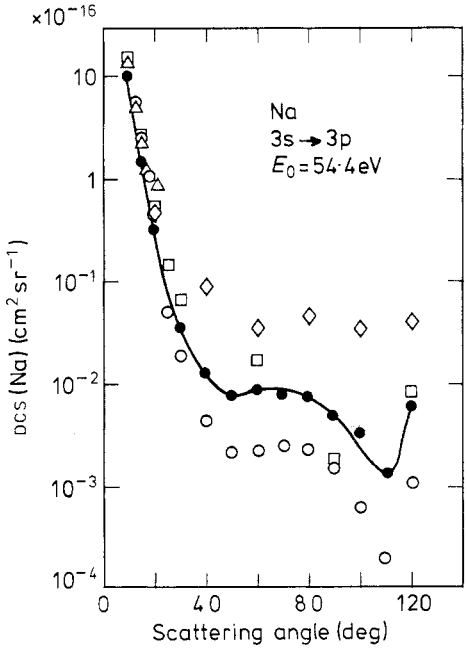

Figure 5. DCS for the electron impact excitation of $3^2S \rightarrow 3^2P$ state in Na for 54·4 eV electrons. ○, S J Buckman and P J O Teubner (1978, private communication); ◇, Issa (1977) (50 eV); □, Kennedy *et al* (1977); △, Shuttleworth *et al* (1977a); ●, present results joined by a best visual fit (full curves).

results closer to the present results at higher scattering angles. This is surprising because the close coupling predictions are expected to give better agreement in this angular range.

There are no theoretical or experimental results readily available for the $3^2S \rightarrow 4^2S$ transition. Present cross sections are given in table 3 and shown in figure 6. These results indicate no systematic trends and no general conclusion can be drawn.

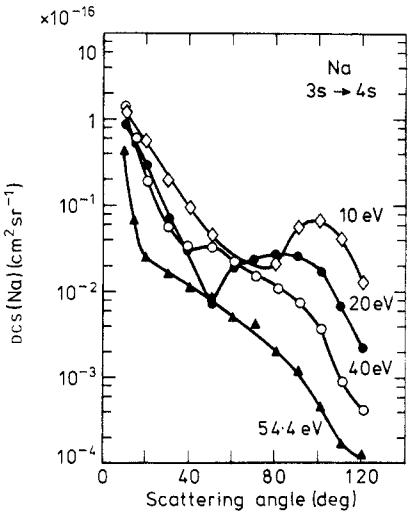

Figure 6. DCS for the electron impact excitation of $3S \rightarrow 4S$ transitions. ◇, $E_0 = 10$ eV; ●, $E_0 = 20$ eV; ○, $E_0 = 40$ eV; and ▲, $E_0 = 54{\cdot}4$ eV. The present results have been joined by the best visual fit (full curves).

Due to poor resolution of the instrument various other transitions could not be resolved. In tables 4 and 5 cross sections are presented for the $3^2S \rightarrow 3^2D + 4^2P$, and $3^2S \rightarrow 4^2D + 4^2F + 5^2P + 5^2S$ transitions. Since theoretical or experimental results are not available no comparisons have been made.

Due to the interference by the direct electron beam (primary beam being wide) the DCS values presented in tables 1–5 could not be obtained for angles below 10° for the scattered intensity. Similarly, due to mechanical problems measurements could not be made for angles above 120°. Therefore, in order to obtain integral and momentum transfer cross sections for the elastic scattering and inelastic transitions extrapolations to 0° and 180° were made.

For the elastic scattering the relative shapes predicted by the calculations of Issa (1977) were used for the regions between 0° and 10° and 120° and 180°. The integrated cross sections were obtained by using the following relations:

$$\sigma_I = 2\pi \int_0^{\pi} \text{DCS} \sin\theta \, d\theta \tag{2}$$

$$\sigma_M = 2\pi \int_0^{\pi} \text{DCS} \sin\theta (1 - \cos\theta) \, d\theta. \tag{3}$$

The values, so obtained, are given at the bottom of table 1.

For inelastic transitions (except for $3^2S \rightarrow 3^2P$) presented in tables 3–5 no theoretical guides are available. However, Shuttleworth *et al* (1977b) have published ratios of these transitions with respect to the resonance $3^2S \rightarrow 3^2P$ transition for 0° scattering angle. Since, from the present results the DCS values of 0° for the $3^2S \rightarrow 3^2P$ transition

were known (using theoretical calculations for extrapolation to 0°) the DCS values for all other cross sections at 0° could be calculated from these ratios. The 0° and 10° cross sections were joined by a straight line and thus the extrapolation was made in the 0–10° region. However, for the 120–180° region a straight line parallel to the x axis was drawn. Since most contribution comes from the 0–120° angular region, this procedure for the high-angle extrapolation did not introduce a large error in the final results. The values for σ_I and σ_M are shown at the bottom of tables 3–5. In table 2 the σ_I values are of Enemark and Gallagher (1972) used for normalisation of the present data and σ_M values have been calculated using equation (3). Errors in σ_I are estimated to be about 30% and about 35% for σ_M.

Table 6 summarises the integral cross sections for various transitions measured either by us or by other workers. These include the cross sections for the $3^2S \rightarrow 3^2P$ transition (Enemark and Gallagher 1972) and for ionisation ($e + Na \rightarrow Na^+ + 2e$) by McFarland and Kinney (1965) and Zapesochnyi and Eleksakhin (1969) reported in 'Atomic Data for Controlled Fusion Research' (1977). By adding the first six columns we obtain total cross sections which are presented in the seventh column. It is evident from this table that the major contribution to the total cross sections comes from elastic scattering and scattering from the first resonance transition ($3^2S \rightarrow 3^2P$). In figure 7 these total cross sections are compared with the measurements of Kasdan *et al* (1973) and the theoretical predictions of Walters (1976) which are based on the Glauber approximation. We have also included the estimation of Bransden and McDowell (1978) who added the elastic cross sections of Issa (1977), 3s–3p cross sections of Enemark and Gallagher (1972), and the cross sections for all other excited states of

Table 6. Integral cross sections for transitions from the ground state (3^2S) to various excited states in Na in units of 10^{-16} cm^2. Total cross sections are the sum of all cross sections.

E_0	Elastic	3^2P[a]	4^2S	3^2D+4^2P	4^2D+4^2F $+5^2P+5^2S$	Ionisation[b]	Total Present
10	43	31·7	1·0	4·3	1·6	6·3	87·9
20	14	29·0	0·52	2·4	0·97	6·5	53·4
40	11	21·8	0·58	2·4	0·87	5·2	41·9
54·4	5·4	18·6	0·30	0·97	0·30	4·7	30·2

[a] Enemark and Gallagher (1972). The values quoted here have been obtained by interpolating their results.
[b] McFarland and Kinney (1965). Zapesochnyi and Aleksakhin (1969).

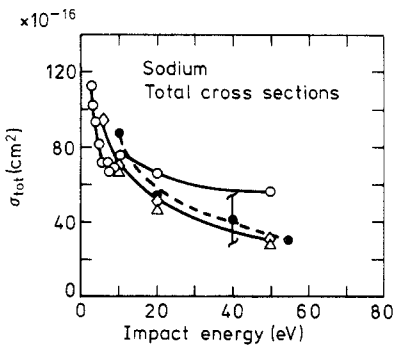

Figure 7. Total electron impact excitation cross sections for Na. ○, Kasdan *et al* (1973); ◇, Walters (1976) (theory); △, Bransden and McDowell (1978) (estimated); ●, present results. All results have been joined by the best visual fit (full curves).

Korff *et al* (1970). As is evident from this figure, our results are in much better agreement with the theoretical predictions. Our estimated error is about 30% and is indicated in the figure for the 40 eV point.

Acknowledgments

The authors are grateful to Dr S Trajmar for valuable discussions during the progress of this research. One of us (SKS) would like to thank Dr W H Williams for providing some preliminary results on Na and for setting up the basic experimental arrangement used in the present measurements.

References

Bransden B H and Coleman J P *J. Phys. B: Atom. Molec. Phys.* **5** 537–45
Bransden B H and McDowell M R C 1978 *Phys. Rep.* **46** 250–394
Enemark E A and Gallagher A 1972 *Phys. Rev.* A **6** 192–205
Gehenn W and Reichert E 1972 *Z. Phys.* **254** 28–34
Issa M R 1977 *PhD Thesis* University of Durham
Kasdan A, Miller T M and Bederson B 1973 *Phys. Rev.* A **8** 1562–9
Kennedy J V, Myerscough V P and McDowell M R C 1977 *J. Phys. B: Atom. Molec. Phys.* **10** 3759–79
Korff D F, Chung S and Lin C C 1973 *Phys. Rev.* A **7** 545–56
McFarland R H and Kinney J D 1965 *Phys. Rev.* **137** A1058–61
Shuttleworth T, Newell W R and Smith A C H 1977a *J. Phys. B: Atom. Molec. Phys.* **10** 1641–51
—— 1977b *J. Phys. B: Atom. Molec. Phys.* **10** 3307–21
Teubner P J O, Buckman S J and Noble C J 1978 *J. Phys. B: Atom. Molec. Phys.* **11** 2345–54
Trajmar S and Brinkmann R 1979 to be published
Trajmar S, Williams W and Srivastava S K 1977 *J. Phys. B: Atom. Molec. Phys.* **10** 3323–33
Williams W and Trajmar S 1977 *J. Phys. B: Atom. Molec. Phys.* **10** 1955–66
Walters H R J 1976 *J. Phys. B: Atom. Molec. Phys.* **9** 227–37
Zapesochnyi I P and Aleksakhin I S 1969 *Sov. Phys.-JETP* **28** 41–4